Aerospace Science and Technology ••• (••••) •••–•••

Contents lists available at ScienceDirect

Aerospace Science and Technology

www.elsevier.com/locate/aescte

An applicable formula for elastic buckling of rectangular plates under biaxial and shear loads

A. Jahanpour *, F. Roozbahani

Department of Civil Engineering, Malayer University, Malayer, Iran

ARTICLE INFO

Article history:
Received 12 May 2016
Received in revised form 1 July 2016
Accepted 12 July 2016
Available online xxxx

Keywords:
Elastic buckling
Rectangular plate
Simply supported
Rayleigh–Ritz method
Biaxial/shear loads

ABSTRACT

As thin plates have relatively big thickness ratios, their elastic buckling usually occurs before the yielding. From beginning of the previous century, many researchers have considered various in-plane loading states on thin plates and have strived to find simple equations to predict the buckling load. However, there are few valid equations with negligible errors for a thin plate, when it is under all of in-plane loads. In this paper, using energy method, an applicable formula is suggested for a simply supported rectangular plate, which is under biaxial and shear loads. The biaxial loads can be applied in the compressive/compressive, compressive/tensile, and tensile/tensile states on the plate. Generally, 15 129 examples are considered for this problem. The aspect ratio of plates varies from 1 to 5 and for each case and with the known load ratios, the plate buckling coefficient is calculated. Then, by using the regression techniques and interpolation, it is tried to estimate a simple equation with minimum error to predict the buckling load. The confirmed results show that for the biaxial compression and shear state, the maximum error is 8% and for the compression–tension–shear and biaxial tension and shear states, it increases until 20%.

1. Introduction

Thin-plated structures are widely used in various engineering industries such as building, bridge, aerospace, marine, shipbuilding and so on. Thin plates usually have thickness ratio between 10 and 100 and in practical purposes they mostly buckle under in-plane axial and shear loading before yielding. Because they have the post-buckling behavior, prediction of the buckling load by an applicable equation with minimum error is very important for such structures.

In many years, the valuable efforts have been performed to find concise equations for the buckling load of flat plates under the various loading types and boundary conditions [1–3]. There are several methods to predict buckling loads of such plates. The older methods have been applied from near the end of the 19th century [1] that mostly included the method of integration of the differential equation and also, the energy method. Recently, the numerical methods have been considered as useful tools for the complicated problems. Generally, the exact solutions can be developed, when the plate is under uniformly distributed compressive in one direction or two perpendicular directions. For the latter state, Lebove [4] showed that one of half-waves in the buckled plate is always unit; but the other one can be achieved by an explicit solution.

In this way, numerous researchers have investigated other states of loadings and boundary conditions through the years. Using energy method, van der Neut [5] obtained the buckling load of a simply supported plate under a half-sine load distribution on the opposite sides and later Benoy [6] investigated this problem for a parabolic distribution. He considered four boundary conditions of plate: (i) ends and sides simply supported, (ii) ends clamped, sides SS, (iii) ends SS, sides C, and (iv) ends and sides C. Also, the loading was expressed in terms of the stresses at the panel edges and center. Benoy compared the obtained results with those of van der Neut. Later, Bert et al. [7] claimed that two previous works were based on an incorrect in-plane stress distribution. They used Galerkin solution to remove the existing deficiencies in the previous works, especially for a sinusoidal stress distribution and then, achieved more accurate results for the buckling load. They concluded that their analysis shows the buckling loads at higher plate aspect ratio increase relative to those obtained in the literature.

Bank and Yin [8] considered buckling of an orthotropic plate, simply supported on its loaded edges and free and rotationally restrained on its unloaded edges. Uniform uniaxial compression was applied on the loaded edges and the method of integration of the differential equation (exact solution) for the deflected plate was used. In this study, the effect of orthotropic properties of the plate material, the plate aspect ratio, the rotational restraint of the one

* Corresponding author. Fax: +988132221977.
E-mail addresses: a.jahanpour@malayeru.ac.ir (A. Jahanpour), farhadroozbahani65@gmail.com (F. Roozbahani).

http://dx.doi.org/10.1016/j.ast.2016.07.005
1270-9638/

loaded edge and the buckle half-wavelength was discussed. They showed that in the case of a plate with a free edge, the Poisson ratio appears explicitly in the boundary conditions. Finally, the buckling curves were presented for the results of parametric studies as well as typical composite materials.

Kang and Leissa [9] presented an exact solution for the buckling and free vibration of rectangular plates having two opposite edges simply supported, each subjected to an in-plane moment, with the other two edges being free. The exact solution was applied in term of an infinite power series, so that sufficient number of terms of the series must be taken to obtain accurate numerical results. The results showed that the critical buckling moment always occurs for a mode having one half-wave in the direction of loading and also, the buckling and frequency parameters depend upon the Poisson ratio. Furthermore, the used approach may be applied equally well to plates having other continuous boundary condition along their unloaded edges.

Elangovan and Prinsze [10] arranged a finite element shear buckling analysis with NASTRAN for flat rectangular plates with two free opposite edges and the other two edges with different boundary conditions. In some curves, the shear buckling coefficient which obtained for the boundary conditions was compared and emphasized that the in-plane flexibility of the supports is an important parameter in the structural design.

In recent decades, the numerical methods have been extended to increase the efficiency and ability. Sherbourne and Pandey [11] used differential quadrature method (DQM) for solving directly the partial differential equation governing the problem with prescribed boundary conditions. This method suggests polynomial approximations of partial derivatives of a function. They employed DQM to compare some examples and results with available standard solutions. Their experience showed that compactness and computational economy of the DQ model are praiseworthy. Later, Civalek [12] compared the methods of differential quadrature (DQ) and harmonic differential quadrature (HDQ). He used these methods for various analysis of thin isotropic plates and columns. Unlike DQ that uses the polynomial functions, HDQ uses harmonic or trigonometric functions as the test functions. Civalek applied both of methods on some examples such as elastic columns, circular, rectangular, skew, trapezoidal, eccentric sectorial, and square plates. He concluded that in the numerical examples, the results obtained with HDQ method are more accurate than the values calculated by using finite elements and finite differences and needs less grid points than the DQ method.

Liew et al. [13] formulated the radial point interpolation method (RPIM) for the buckling analysis of non-uniformly loaded thick plate. The RPIM is a mesh-free method, so that the problem domain is not divided into sub-domain to approximate the displacement (unlike the FEM). The buckling loads of the circular, trapezoidal and skew plates were calculated and compared with FEM. Furthermore, Civalek et al. [14] used discrete singular convolution (DSC) for buckling and free vibration analyses of rectangular plates subjected various in-plane compressive loads and with different boundary conditions. The mathematical foundation of this method is the theory of distributions and wavelet analysis. The obtained results were compared with those of other numerical methods.

Beyond the described investigations, many studies can be found that have been presented for buckling of thin plates under combinations of in-plane loads and various boundary conditions. Using energy method, McKenzie [15] gave an analysis of the buckling of a rectangular plate of arbitrary aspect ratio under combination of biaxial compression, bending and shear. In this investigation, the pair of sides of the plate to which bending is applied are assumed to be simply supported, while the other two sides are supported by edges members of arbitrary torsional and flexural stiffnesses. McKenzie generated some interaction curves for different aspect ratios and load ratios.

Liu and Pavlovic [16] broke-down external loads (direct, shear and bending loads) into four parts in the symmetrical and anti-symmetrical forms. For a simply supported rectangular plate and using principle of super position, the Ritz energy technique was used to compute the buckling coefficient of the plate. They emphasized that the proposed approach based on formal plane stress elasticity solution enables the true distribution in any plate to be obtain irrespective of the complexity and/or arbitrariness of applied forced on any edges.

However, some equations have been approximately developed among pure shear, pure bending, combined shear and longitudinal compression, shear and bending load [17–19]. Although a few investigations can be found for the buckling behavior of plates under biaxial and shear loads, Wagner [20–22] established two formulas to calculate the critical shear stress of simply supported and clamped plates with given values of biaxial stresses:

$$\left(\frac{\tau_{crm}}{\tau_0}\right)^2=\left(2\sqrt{1-\frac{\sigma_y}{\tau_0}}+2-\frac{\sigma_x}{\tau_0}\right)\left(2\sqrt{1-\frac{\sigma_y}{\tau_0}}+6-\frac{\sigma_x}{\tau_0}\right);$$
all edges simply supported
$$\left(\frac{\tau_{crm}}{\tau_0}\right)^2=\left(2.31\sqrt{4-\frac{\sigma_y}{\tau_0}}+\frac{4}{3}-\frac{\sigma_x}{\tau_0}\right)\left(2.31\sqrt{4-\frac{\sigma_y}{\tau_0}}+8-\frac{\sigma_x}{\tau_0}\right);$$
all edges clamped (1)

where

$$\tau_0=\frac{\pi^2 E}{12(1-\upsilon^2)}\left(\frac{t}{b}\right)^2$$

In above equation, σ_x and σ_y are axial stresses in x- and y-directions respectively. They have negative values when are tensile. To use this equation, the plate aspect ratio must be very large [22]. As a result, Eqs. (1) could not be used for usual aspect ratio of plates ($1<\alpha<5$).

Chen et al. [23] estimated a concise formula for the critical buckling stresses of an elastic plate under biaxial compression and shear (Eq. (2)). They considered the plate aspect ratio between 1 and 5.

$$\frac{\sigma_x}{\sigma_{x,cr}}+\left(\frac{\sigma_y}{\sigma_{y,cr}}\right)^\gamma+\left(\frac{\tau_{crm}}{\tau_{cr}}\right)^2=1 \tag{2}$$

where

$$\gamma=\begin{cases}1; & 1\le\alpha\le\sqrt{2}\\ \alpha^{[1-(\frac{\tau_{crm}}{\tau_{cr}})^2]}; & \alpha>\sqrt{2}\end{cases}\quad;\quad \alpha=\frac{a}{b}$$

In Eq. (2), σ_x is compressive stress in x-direction; $\sigma_{x,cr}$ is uniaxial compressive buckling stress in x-direction; σ_y is compressive stress in y-direction; $\sigma_{y,cr}$ is uniaxial compressive buckling stress in y-direction; τ_{crm} is modified shear buckling stress of the plate and τ_{cr} is pure shear buckling stress of the plate.

Chen et al. emphasized that the maximum error of the critical stress relationship in above equation is found to be less than 0.5% for $1\le\alpha<\sqrt{2}$, 5% for $\sqrt{2}\le\alpha<2$, and 10% for $2\le\alpha<5$ [23]. Eq. (2) shows that for $\alpha>\sqrt{2}$, without shear load ($\tau_{crm}=0$), $\gamma=\alpha$. As a result, Eq. (2) is converted to $\frac{\sigma_x}{\sigma_{x,cr}}+(\frac{\sigma_y}{\sigma_{y,cr}})^\alpha=1$. It can be shown that for the biaxial loaded plates, power of both of the terms must be unit [1,22], whereas here $\alpha>\sqrt{2}$.

In addition, according to Von-Mises criteria, DNV-RP-C201 has an equation which can be used to obtain inelastic buckling of unstiffened plate under biaxial compression and shear loads [24].

Please cite this article in press as: A. Jahanpour, F. Roozbahani, An applicable formula for elastic buckling of rectangular plates under biaxial and shear loads, Aerosp. Sci. Technol. (2016), http://dx.doi.org/10.1016/j.ast.2016.07.005

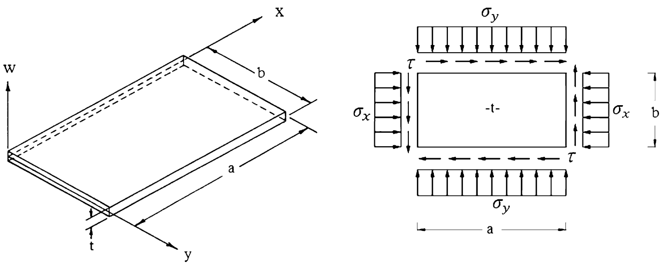

Fig. 1. A simply supported rectangular plate with $a \times b \times t$ dimensions under compression biaxial and shear stresses.

In this paper, the Rayleigh–Ritz method is applied on simply supported thin rectangular plates with aspect ratio between 1 and 5 to achieve the coefficient of elastic buckling load for three types of in-plane loading: compression–compression–shear, compression–tension–shear and tension–tension–shear. Then, using the regression technique and interpolation, an applicable equation with relatively acceptable accuracy is represented to predict the buckling load of plates. The number of half-waves of buckled plate under biaxial loading is an essential stage for above calculations. The obtained results are validated with those of the Rayleigh–Ritz method and the finite element modeling. Finally, the appeared errors from each type of loading are represented.

2. The analytical method

2.1. The Rayleigh–Ritz approach [2]

For a rectangular plate with known boundary and loading conditions (Fig. 1), initially, the total potential energy function must be established (Eq. (3)) and then minimized. This function has two parts: the total strain energy (Eq. (4)) and the external forces potential functions (Eq. (5)). The latter function is calculated for a plate that is under biaxial and shear stresses.

$$\Pi = U - V \tag{3}$$

$$U = \frac{D}{2}\int_0^a\int_0^b\left[\left(\frac{\partial^2 w}{\partial x^2}+\frac{\partial^2 w}{\partial y^2}\right)^2 - 2(1-\nu)\left(\frac{\partial^2 w}{\partial x^2}\frac{\partial^2 w}{\partial y^2}\right.\right.$$
$$\left.\left. - \left(\frac{\partial^2 w}{\partial x \partial y}\right)^2\right)\right]dxdy \tag{4}$$

$$V = \frac{t}{2}\int_0^a\int_0^b\left[\sigma_x\left(\frac{\partial w}{\partial x}\right)^2 + \sigma_y\left(\frac{\partial w}{\partial y}\right)^2\right.$$
$$\left. - 2\tau_{xy}\left(\frac{\partial w}{\partial x}\frac{\partial w}{\partial y}\right)\right]dxdy \tag{5}$$

where t is the plate thickness and D is bending rigidity of the plate that calculated as below:

$$D = \frac{Et^3}{12(1-\nu^2)} \tag{6}$$

where E is module of elasticity and ν is Poisson ratio of the plate material. In Eqs. (4) and (5), w is a double sine function to show the plate displacement, so that it satisfies the boundary conditions (Eq. (7)):

$$w(x,y) = \sum_{m=1}^{\infty}\sum_{n=1}^{\infty} A_{mn}\sin\frac{m\pi x}{a}\sin\frac{n\pi y}{b} \tag{7}$$

where m and n are number of the half-waves that appear in x and y directions respectively and A_{mn} is unknown coefficient. Substituting Eq. (7) in Eqs. (4) and (5), the functions of U and V can be simplified as below:

$$U = \frac{Dab\pi^4}{8}\sum_{m=1}^{\infty}\sum_{n=1}^{\infty}A_{mn}^2\left(\frac{m^2}{a^2}+\frac{n^2}{b^2}\right)^2 \tag{8}$$

$$V = \frac{\pi^2 abt}{8}\sum_{m=1}^{\infty}\sum_{n=1}^{\infty}A_{mn}^2\left[\sigma_x\frac{m^2}{a^2}+\sigma_y\frac{n^2}{b^2}\right]$$
$$-4t\tau\sum_{m=1}^{\infty}\sum_{n=1}^{\infty}\sum_{p=1}^{\infty}\sum_{q=1}^{\infty}A_{mn}A_{pq}\frac{mnpq}{(m^2-p^2)(n^2-q^2)} \tag{9}$$

In Eq. (9), $(m+p)$ and $(n+q)$ must be odd numbers, thus $(m+n+p+q)$ must be even, i.e. $m+n$ and $p+q$ must be even or odd numbers simultaneously. A set of equations can be achieved to minimize the total potential energy function that shown in Eqs. (10):

$$\left(\frac{\partial \Pi}{\partial A_{mn}}\right) = \frac{\partial(U-V)}{\partial A_{mn}} = 0;$$
$$m = 1,2,3,\ldots,M;\; n = 1,2,3,\ldots,N \tag{10}$$

where M and N are the minimum terms that must be selected to find convergence in the results. Substituting Eqs. (8) and (9) in Eqs. (10), the set of equations can be simplified as shown in Eq. (11):

$$A_{mn}\left[\left(m^2+n^2\alpha^2\right)^2 - k_x m^2\alpha^2 - k_y n^2\alpha^4\right]$$
$$+\frac{32k_s\alpha^3}{\pi^2}\sum_{p=1}^{\infty}\sum_{q=1}^{\infty}A_{pq}\frac{mnpq}{(m^2-p^2)(n^2-q^2)} = 0 \tag{11}$$

where

$$\begin{cases} k_x = \dfrac{tb^2}{D\pi^2}\sigma_x \\ k_y = \dfrac{tb^2}{D\pi^2}\sigma_y \\ k_s = \dfrac{tb^2}{D\pi^2}\tau \end{cases} \tag{12}$$

In Eqs. (11) and (12), k_x, k_y and k_s are the coefficients of critical stress in x, y and xy directions respectively and $\alpha = a/b$ is the plate aspect ratio (Fig. 1). As a general closed-form solution could not be found for the set of Eqs. (11), the limited terms must be selected. Therefore, a set of $M \times N$ linear equations for the unknown coefficients of A_{mn} are established that can be shown in matrix form (Eq. (13)):

$$[C]_{L\times L}\{A\}_{L\times 1} = 0; \quad L = M \times N \tag{13}$$

It can be shown that considering $M = N = 10$, the results are found with successful convergence [25]. The different dimensionless parameters, $R = \frac{\sigma_y}{\tau} = \frac{k_y}{k_s}$ and $S = \frac{\sigma_x}{\tau} = \frac{k_x}{k_s}$, and the plate aspect ratio are considered as below:

$$\alpha = 1, 1.1, 1.2, 1.3, \ldots, 4.8, 4.9 \text{ and } 5$$

$$S = -1, -0.8, -0.6, -0.4, -0.2, -0.1, 0, 0.1, 0.2, 0.4, 0.6, 0.8,$$
$$1, 1.2, 1.5, 2, 3, 4, 5 \text{ and } 10$$

$$R = -1, -0.8, -0.6, -0.4, -0.2, -0.1, 0, 0.1, 0.2, 0.4, 0.6, 0.8,$$
$$1, 1.2, 1.5, 2, 3, 4, 5 \text{ and } 10$$

Please cite this article in press as: A. Jahanpour, F. Roozbahani, An applicable formula for elastic buckling of rectangular plates under biaxial and shear loads, Aerosp. Sci. Technol. (2016), http://dx.doi.org/10.1016/j.ast.2016.07.005

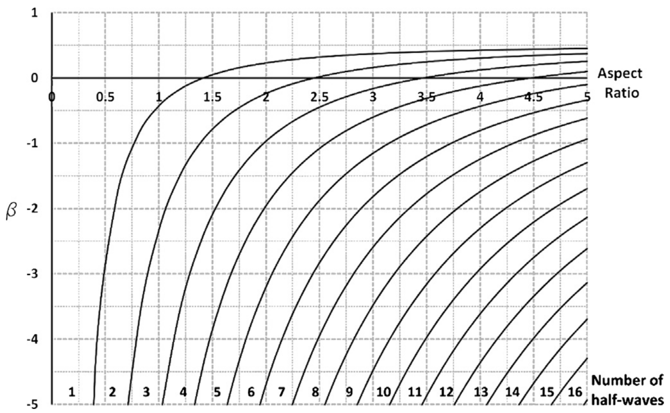

Fig. 2. The boundary curves between consecutive buckling modes for the biaxial loaded plate.

where negative sign refers to tensile stresses. All load cases are $S \times R = 20 \times 20 = 400$. In some load cases, it is possible that the plate yielding occurs before the elastic buckling. Therefore, such states must be eliminated from above arrangement and the number of load cases are reduced to 369. Finally, all examples are realized as $369 \times 41 = 15\,129$. Eq. (13) is solved for all examples and the buckling coefficient is determined for each case. The comparison between the obtained results and finite element models show that the biaxial loading state (without shear stresses) has major influence on the number of half-waves in the buckled plate and they have small dependence to the shear stresses. In the following, this state is applied to find them.

2.2. Calculation of the number of half-waves for the biaxial loading

If there is no shear stress on the plate, Eq. (11) has the closed-form solution as shown in Eq. (14) [1]:

$$\sigma_x = k_x \frac{D\pi^2}{tb^2}; \qquad k_x = \frac{\left[\left(\frac{m}{\alpha}\right)^2 + n^2\right]^2}{\left[\left(\frac{m}{\alpha}\right)^2 + \beta n^2\right]} \tag{14}$$

where $\beta = \frac{\sigma_y}{\sigma_x}$ is the axial loads ratio. It has been shown that one of the half-waves is always unit [4] (Here, it is supposed that $n = 1$). As m is an integer number, using Eq. (15), the relationship among α and β can be found in the boundary between mth and $(m+1)$th half-waves as shown in Eq. (16).

$$\frac{\left[\left(\frac{m}{\alpha}\right)^2 + 1\right]^2}{\left(\frac{m}{\alpha}\right)^2 + \beta} = \frac{\left[\left(\frac{m+1}{\alpha}\right)^2 + 1\right]^2}{\left(\frac{m+1}{\alpha}\right)^2 + \beta} \tag{15}$$

$$\beta = \frac{\alpha^4 - m^2(m+1)^2}{\alpha^2[2\alpha^2 + (m+1)^2 + m^2]} \tag{16}$$

Fig. 2 shows Eq. (16) graphically in the different buckling modes ($\alpha \geq 1$). As pointed, one of the half-waves is permanently unit and using Fig. 2, with both known parameters (α and β), the number of half-waves in other direction can be achieved. In Fig. 2 and for negative β, it is always supposed that $\sigma_x > 0$ and $\sigma_y < 0$. For the opposite state, the plate and its applied stresses must be rotated in 90° to reach to above conditions. As a result, the inversed α and β must be considered. In this situation, $m = 1$ and n is determined from Fig. 2. For example, if $\beta = -3$, $\alpha = 1.5$, $\sigma_x < 0$ and $\sigma_y > 0$, after rotation of the plate, the new values of α and β are found as 0.67 and -0.333 respectively. Using Fig. 2, $n = 1$ can be attained (and $m = 1$). But, if $\sigma_x > 0$ and $\sigma_y < 0$, there is no change for α and β, so that $m = 4$ (and $n = 1$). When both of σ_x and σ_y are applied as tensile stresses, apart from Eq. (15), it is supposed that both of the half-waves are unit ($m = n = 1$).

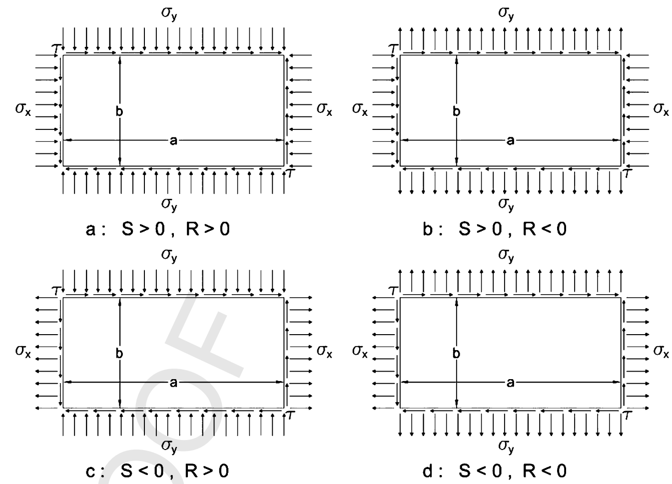

Fig. 3. The different states of in-plane loading on the plate.

2.3. Estimation of a suitable equation for the obtained data

To predict an appropriate function that can evaluate the plate buckling coefficient with minimum error, the regression and interpolation methods are used. In this way, package GeneXproTools [26] is widely employed and thousands functions are examined with different interpolators. Finally, the best function with the least error is obtained as below:

$$k_x = \frac{\left[\left(\frac{m}{\alpha}\right)^2 + n^2\right]^2}{\left[\left(\frac{m}{\alpha}\right)^2 + \beta n^2\right]} . \delta \tag{17}$$

where δ is a coefficient that is additionally introduced to Eq. (14) when shear load is added to the biaxial loaded plate. It is defined as below:

$$\delta = \begin{cases} 1 - \left(\frac{k_s}{k_{s,cr}}\right)^2; & \left(\frac{k_s}{k_{s,cr}}\right) < 0.25 \text{ or } \alpha \leq 1.6 \\ e^{\frac{\alpha\beta}{20} \cdot \left(\frac{k_s}{k_{s,cr}}\right)^2} - \left(\frac{k_s}{k_{s,cr}}\right)^2; & \left(\frac{k_s}{k_{s,cr}}\right) \geq 0.25 \text{ and } \alpha > 1.6 \end{cases} \tag{18}$$

After simplification, Eq. (17) can be converted as shown below:

$$\frac{k_x}{k_{x,cr}} + \frac{k_y}{k_{y,cr}} + \left(\frac{k_s}{k_{s,cr}}\right)^2 = \lambda$$

$$\lambda = \begin{cases} 1; & \left(\frac{k_s}{k_{s,cr}}\right) < 0.25 \text{ or } \alpha \leq 1.6 \\ e^{\frac{\alpha\beta}{20} \cdot \left(\frac{k_s}{k_{s,cr}}\right)^2}; & \left(\frac{k_s}{k_{s,cr}}\right) \geq 0.25 \text{ and } \alpha > 1.6 \end{cases} \tag{19}$$

where $k_{x,cr}$ and $k_{y,cr}$ are coefficients of uni-axial critical stresses with half-waves corresponding to the biaxial state in x- and y-directions respectively (Eqs. (20) and (21)). These half-waves should be obtained from Fig. 2 (Eq. (16)). Also, $k_{s,cr}$ is that of pure shear which obtained from Eq. (22).

$$k_{x,cr} = \frac{\left[\left(\frac{m}{\alpha}\right)^2 + n^2\right]^2}{\left(\frac{m}{\alpha}\right)^2} \tag{20}$$

$$k_{y,cr} = \frac{\left[\left(\frac{m}{\alpha}\right)^2 + n^2\right]^2}{n^2} \tag{21}$$

$$k_{s,cr} = 5.34 + \frac{4}{\alpha^2} \tag{22}$$

Eq. (19) is suitable for compression–compression–shear state (Fig. 3a). If there is at least one tension (negative) stress (Fig. 3b–d), then λ is always considered unit and the shear buckling coefficient (k_s), is always calculated from Eq. (23):

Please cite this article in press as: A. Jahanpour, F. Roozbahani, An applicable formula for elastic buckling of rectangular plates under biaxial and shear loads, Aerosp. Sci. Technol. (2016), http://dx.doi.org/10.1016/j.ast.2016.07.005

Table 1
The different zones in presence of the tensile stresses with possible modifier factors (Eqs. (24) and (25)).

C–T–S	$S>0$ and $R<0$ (Fig. 3b)	$S \le 1.4$, Zone *I*		$S>1.4$, Zone *II*
		η_1		*None*
	$S<0$ and $R>0$ (Fig. 3c)	$S<-0.4$ and $R \le 1$, Zone *III*		$S \ge -0.4$ or $R>1$, Zone *IV*
		$n=m=1$	$n>1$, $m=1$	*None*
		None	η_2*	
T–T–S**	$S<0$ and $R<0$ (Fig. 3d)	$S<-0.4$ or $R<-0.4$, Zone *V*		$S \ge -0.4$ and $R \ge -0.4$, Zone *VI*
		η_1		*None*

* If $\eta_2 k_s^n < k_s^{n-1}$, then the procedure is correct; otherwise, the shear buckling coefficient is k_s^{n-1}, where k_s^n and k_s^{n-1} are calculated from Eq. (23) for n and $(n-1)$ half-wave(s) respectively.
** The proposed equation has an acceptable prediction, if $|R| \le |S|$.

$$\frac{k_x}{k_{x,cr}} + \frac{k_y}{k_{y,cr}} + \left(\frac{k_s}{k_{s,cr}}\right)^2 = 1 \tag{23}$$

Eq. (23) may be modified by a factor (η_1 or η_2) that should be achieved by Eqs. (24) and (25).

$$\eta_1 = \left(R + |RS + 0.011|\right)^2 - R + |S|^{-0.45|S|(R+R^5)} + \frac{0.91RS}{0.82^{R|S|}} + \frac{\alpha - 1.41}{50} \tag{24}$$

$$\eta_2 = \left(S + |RS + 0.011|\right)^2 - S + |R|^{-0.45|R|(S+S^5)} + \frac{0.91RS}{0.82^{S|R|}} + \frac{\alpha - 1.41}{50} \tag{25}$$

where $S = \frac{k_x}{k_s}$ and $R = \frac{k_y}{k_s}$. Eq. (25) is defined when R is replaced with S in Eq. (24) and vice versa. Table 1 shows the modifier factors (η_1 or η_2) that must be applied on k_s in three situations. In this table, it is supposed that k_s is always positive. This table shows some states which it is not necessary to use η_1 or η_2 and k_s can be directly obtained from Eq. (23). However, in presence of the tensile load(s) it is necessary to check that the elastic buckling occurs before the yielding.

3. Comparison of the results with the Rayleigh–Ritz method

For each loading state which is shown in Fig. 3, the coefficient of buckling (k_x or k_s) is calculated from both of the proposed equation (Eq. (19) or (23)) and the Rayleigh–Ritz method. In C–C–S state (Fig. 3a), it is better that the coefficient 'k_x' is supposed as an unknown variable, because in Eq. (19) the parameter 'λ' is function of 'k_s' in some cases. Thus, if 'k_s' is an unknown variable, the equation must be solved with a trial and error method. However, in T–C–S (Fig. 3b and 3c) and T–T–S (Fig. 3d) states, $\lambda = 1$ identically and there is no significant difference between prediction of k_x and k_s.

3.1. Compression–Compression–Shear state (C–C–S)

Eq. (19) has acceptable accuracy to predict the plate buckling coefficient and the obtained results can compare to those of the energy method. Figs. 4–11 show the comparison between two methods in some loading states and for aspect ratio among 1 to 5. In these figures, the vertical axis shows the buckling stress coefficient of plate in x-direction (k_x). Table 2 shows the maximum and minimum difference between two methods with corresponding aspect ratios which appeared in the presented figures. The figures numbers have been arranged based on the maximum difference increasing. When $k_s/k_x = 0.1$ and $\beta = 1$, the best conformity is seen (Fig. 4). In this loading case, one half-wave always appears in the both of perpendicular directions ($m = n = 1$). In Fig. 5, before $\alpha = 2.8$, there is no significant difference; but in this aspect ratio, it grows once up to 0.8% and after that, it changes smoothly. In

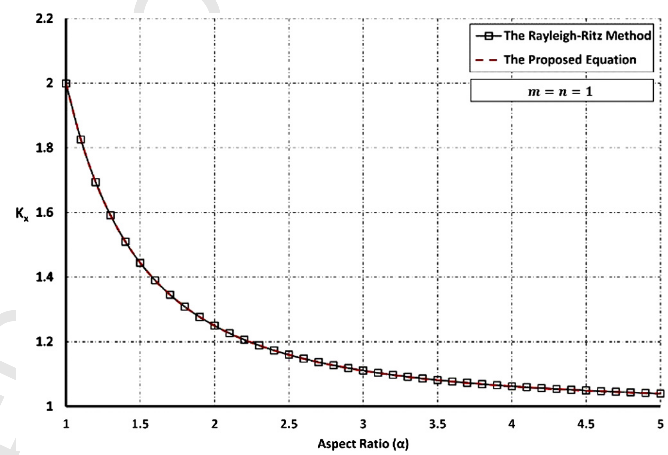

Fig. 4. The k_x–α diagrams for $k_s/k_x = 0.1$ and $\beta = 1$.

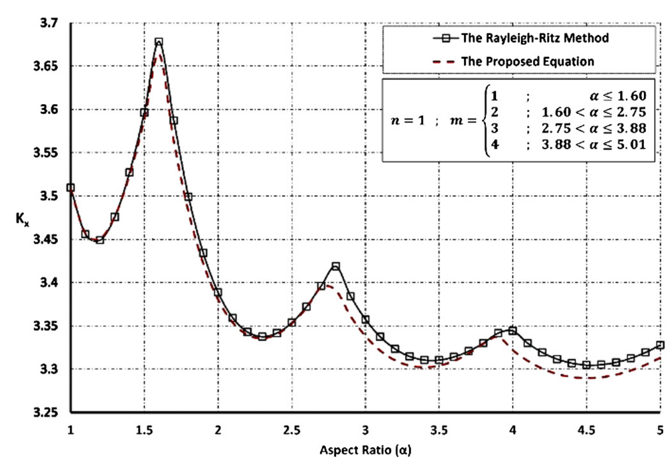

Fig. 5. The k_x–α diagrams for $k_s/k_x = 0.5$ and $\beta = 0.1$.

Fig. 6, very good fitting has been achieved between two diagrams and the difference increases to 1.7% (Table 2). However, there are four buckling modes in Fig. 7 and the maximum difference appears on $m = 4$ and $\alpha = 5$. This figure shows that before $\alpha = 1.4$, the error is very small. In Figs. 8 and 11, using the Rayleigh–Ritz method, the buckling mode changes from $m = 1$ to $m = 2$, when $\alpha = 2.6$ and $\alpha = 2.8$ respectively; but using Eq. (19), for $k_s/k_x = 1$ and $\beta = 0.4$ (Fig. 8), it changes on $\alpha = 3.4$ and consequently, there is 3.5% difference between two methods on $m = 1$ and $\alpha = 2.6$. Furthermore, for $k_s/k_x = 5$ and $\beta = 1$ (Fig. 11), there is always one half-wave in the plate and therefore, 6.7% difference appears. In Figs. 9 and 10, the two methods have relatively good coordination, so that increasing aspect ratio leads to increasing error until it reaches about 4%, when $\alpha = 5$.

Please cite this article in press as: A. Jahanpour, F. Roozbahani, An applicable formula for elastic buckling of rectangular plates under biaxial and shear loads, Aerosp. Sci. Technol. (2016), http://dx.doi.org/10.1016/j.ast.2016.07.005

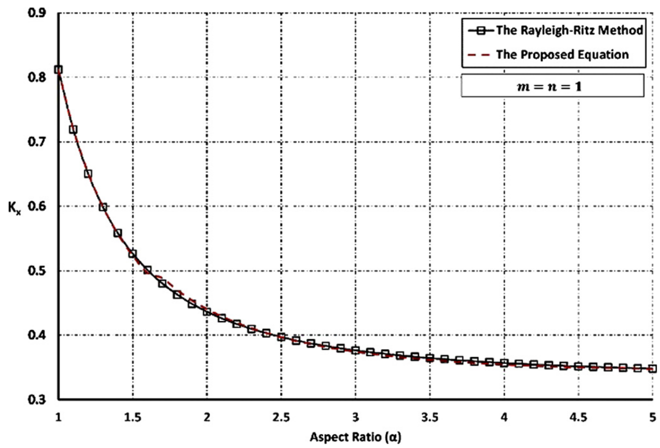

Fig. 6. The k_x–α diagrams for $k_s/k_x = 5$ and $\beta = 3$.

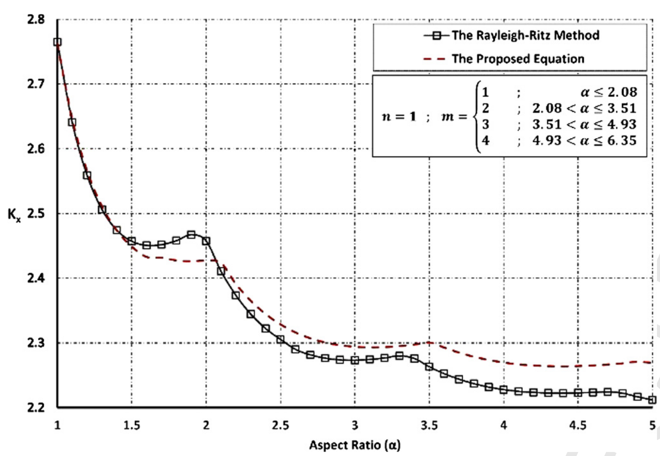

Fig. 7. The k_x–α diagrams for $k_s/k_x = 1.25$ and $\beta = 0.25$.

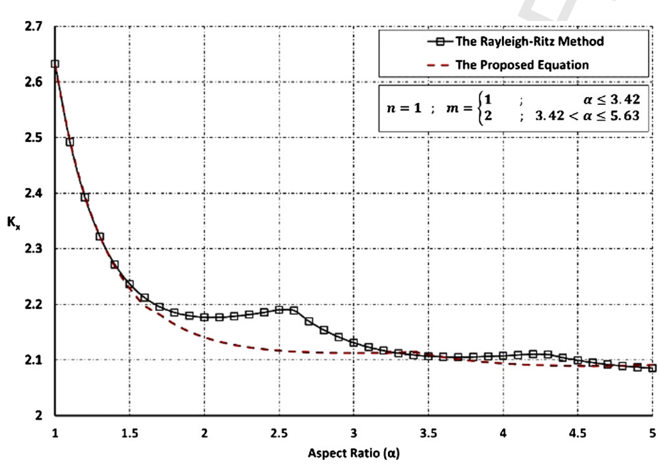

Fig. 8. The k_x–α diagrams for $k_s/k_x = 1$ and $\beta = 0.4$.

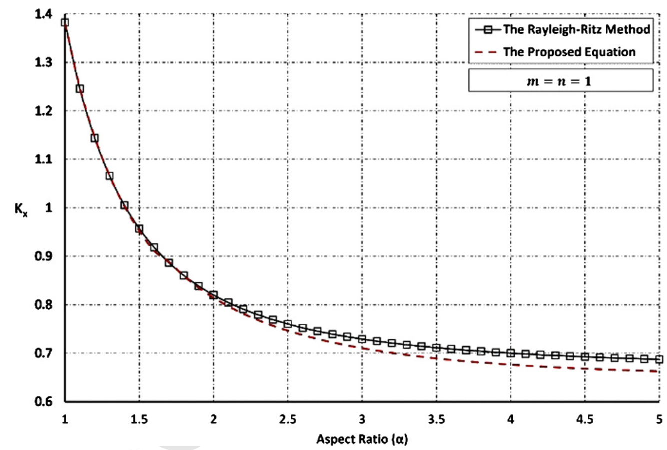

Fig. 9. The k_x–α diagrams for $k_s/k_x = 2.5$ and $\beta = 1.5$.

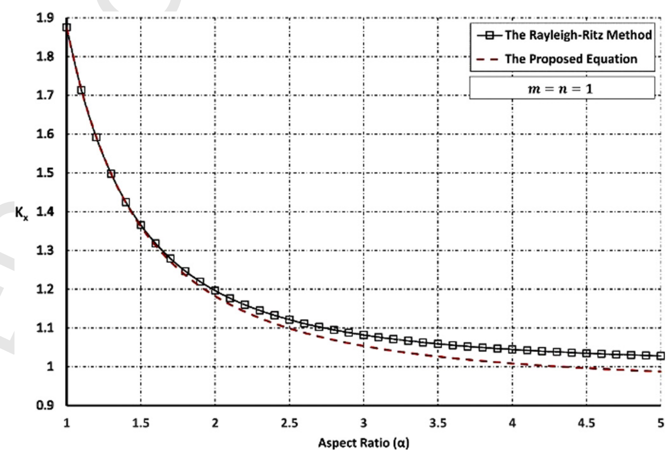

Fig. 10. The k_x–α diagrams for $k_s/k_x = 1.25$ and $\beta = 1$.

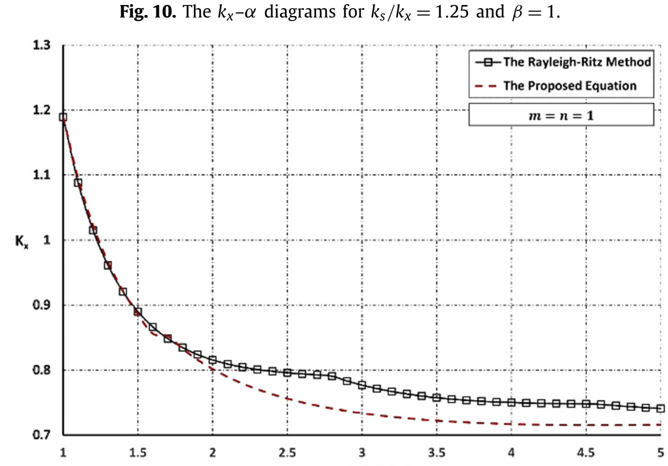

Fig. 11. The k_x–α diagrams for $k_s/k_x = 5$ and $\beta = 1$.

Generally, the shown examples and other loading cases represent that the greater aspect ratio usually leads to the greater errors. In addition, a desirable relationship could not be found between the loadings ratios and the maximum difference. Finally, after comparison among all of obtained results, the maximum difference appeared in Eq. (19), can be summarized in Table 3.

Table 2
Difference between two methods for C–C–S loading.

Figure no.	k_s/k_x	β	Max.			Min.		
			Value (%)	α	m	Value (%)	α	m
4	0.1	1	0.03	5	1	0.0002	1.1	1
5	0.5	1	0.8	2.8	3	0.01	1.3	1
6	5	3	1.7	1.7	1	0.03	1.3	1
7	1.25	0.25	2.5	5	4	0.02	1.4	1
8	1	0.4	3.5	2.6	1	0.02	3.6	2
9	2.5	1.5	3.7	5	1	0.02	1.3	1
10	1.25	1	4.1	5	1	0.01	1.3	1
11	5	1	6.7	2.8	1	0.02	1	1

Please cite this article in press as: A. Jahanpour, F. Roozbahani, An applicable formula for elastic buckling of rectangular plates under biaxial and shear loads, Aerosp. Sci. Technol. (2016), http://dx.doi.org/10.1016/j.ast.2016.07.005

Table 3
The maximum error for the different conditions of C–C–S loading.

Maximum error (%)	The plate conditions
1	$1 \le \alpha < 1.5$
4	$1.5 \le \alpha < 3$
8	$3 \le \alpha \le 5$
1	$\frac{k_s}{k_{s,cr}} \le 0.25$
8	$0.25 < \frac{k_s}{k_{s,cr}} \le 1$

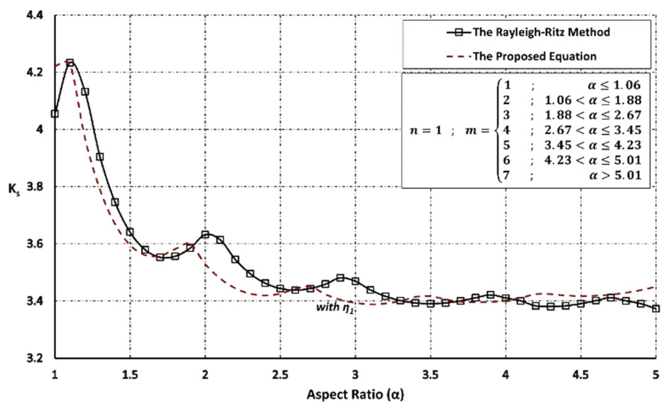

Fig. 12. The k_s–α diagrams for $S = 1.2$ and $R = -0.4$ ($\beta = -0.333$, zone I).

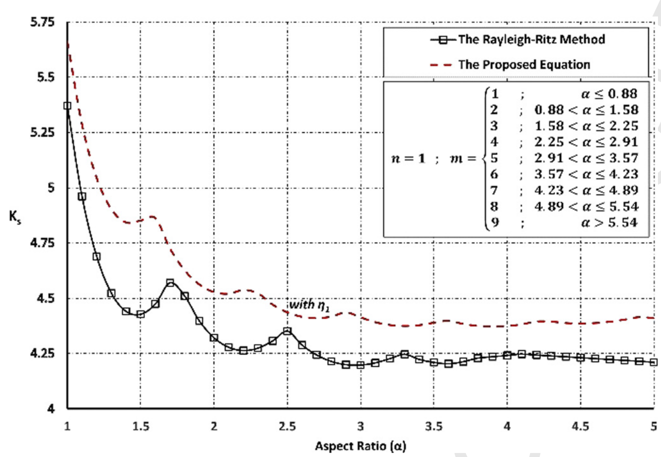

Fig. 13. The k_s–α diagrams for $S = 1.2$ and $R = -0.8$ ($\beta = -0.67$, zone I).

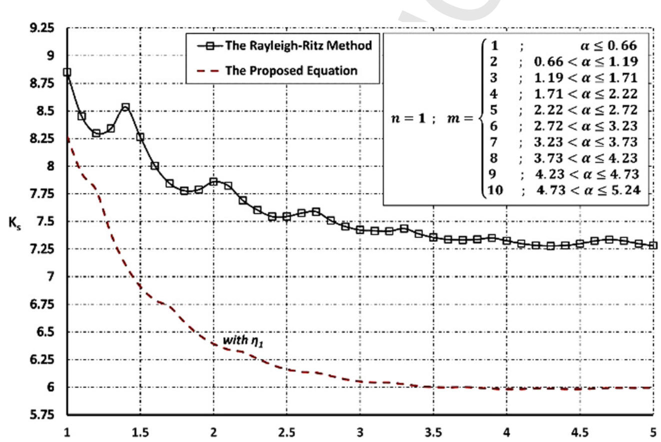

Fig. 14. The k_s–α diagrams for $S = 0.8$ and $R = -1.2$ ($\beta = -1.5$, zone I).

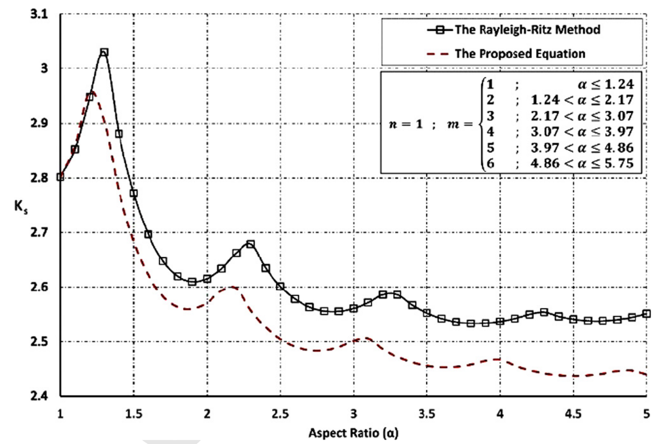

Fig. 15. The k_s–α diagrams for $S = 1.5$ and $R = -0.2$ ($\beta = -0.133$, zone II).

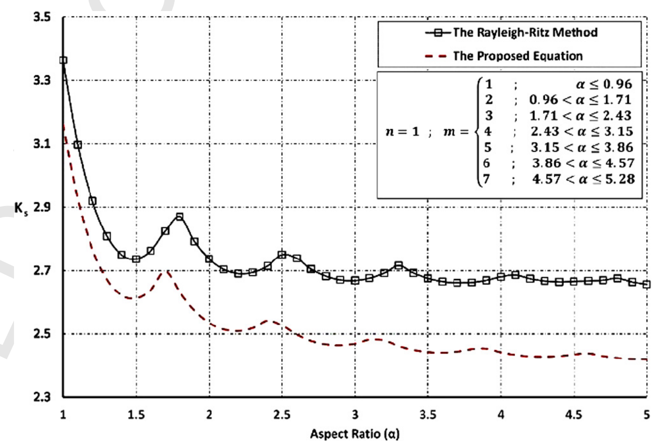

Fig. 16. The k_s–α diagrams for $S = 2$ and $R = -1$ ($\beta = -0.5$, zone II).

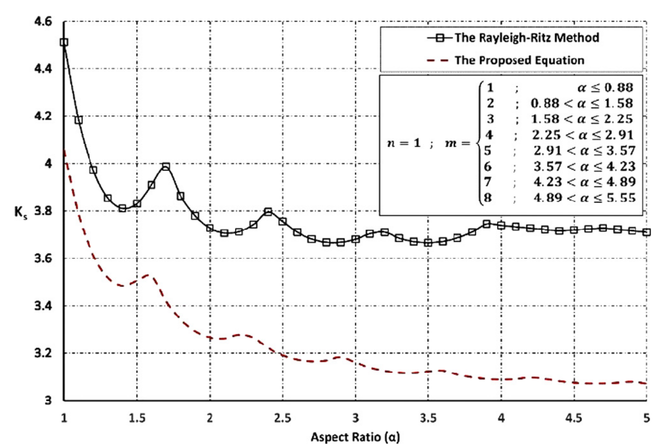

Fig. 17. The k_s–α diagrams for $S = 1.5$ and $R = -1$ ($\beta = -0.667$, zone II).

3.2. Tension–Compression–Shear state (T–C–S)

When one of the applied stresses is tensile and it is applied on the plate length (Fig. 3b), Eq. (23) predicts the satisfactory results, if $\sigma_x > 1.4\tau$. Furthermore, if the tensile stress is applied on the plate width (Fig. 3c), the proposed equation can be used solitarily, if $|\sigma_x| \le 0.4\tau$ or $\sigma_y > \tau$. In the other conditions, Eq. (23) must be modified as shown in Table 1. Figs. 12–23 have been adjusted for zones I to IV respectively that are defined in Table 1. These figures show the comparison between the shear buckling coefficients (k_s) which calculated by two methods in some loading ratios and for aspect ratio among 1 to 5. Also, Tables 4 and 5 represent the

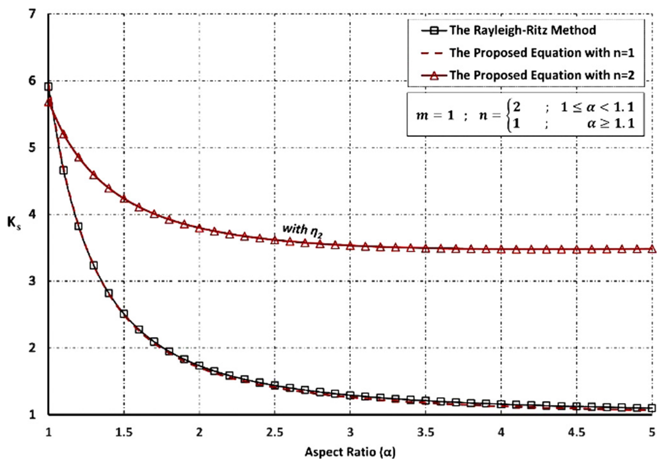

Fig. 18. The k_s–α diagrams for $S=-0.6$ and $R=1$ ($\beta=-1.67$, zone *III*).

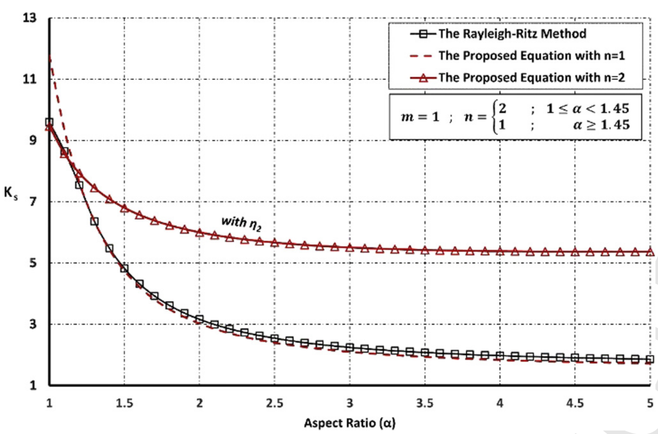

Fig. 19. The k_s–α diagrams for $S=-0.8$ and $R=0.6$ ($\beta=-0.75$, zone *III*).

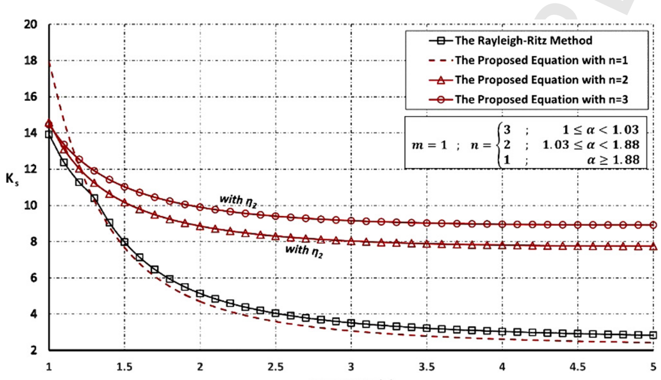

Fig. 20. The k_s–α diagrams for $S=-1$ and $R=0.4$ ($\beta=-0.4$, zone *III*).

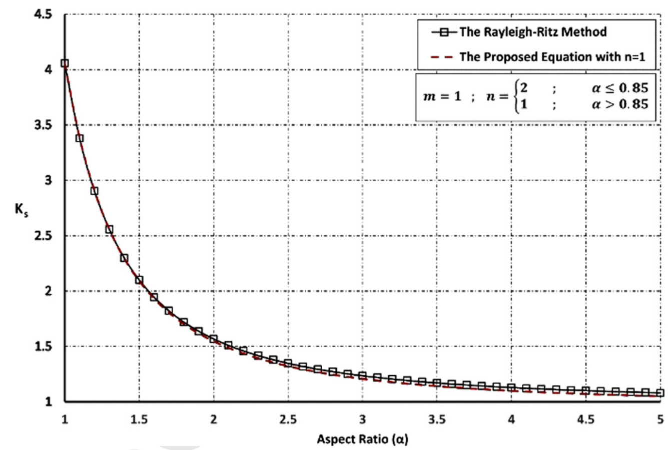

Fig. 21. The k_s–α diagrams for $S=-0.2$ and $R=1$ ($\beta=-5$, zone *IV*).

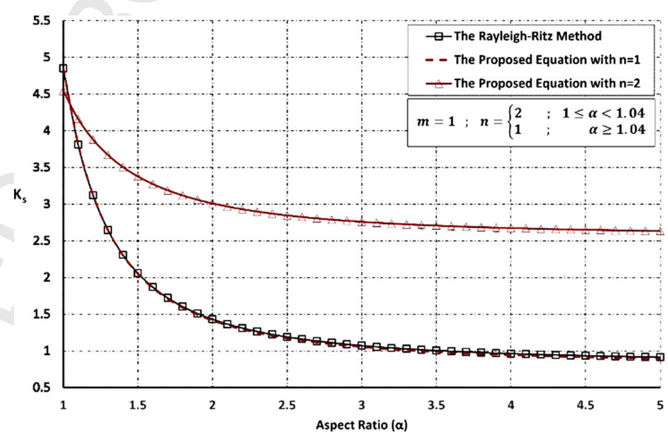

Fig. 22. The k_s–α diagrams for $S=-0.6$ and $R=1.2$ ($\beta=-2$, zone *IV*).

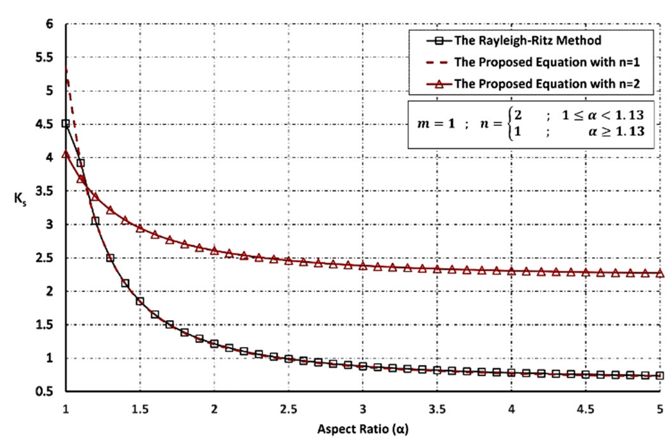

Fig. 23. The k_s–α diagrams for $S=-1$ and $R=1.5$ ($\beta=-1.5$, zone *IV*).

Table 4
Difference between two methods for T–C–S loading (zones *I* and *II*).

Zone	Figure no.	S	R	Max. Value (%)	α	m	Min. Value (%)	α	m
I	12	1.2	−0.4	4.1	1	1	0.05	3.3	4
	13	1.2	−0.8	9.6	1.5	2	2	2.5	4
	14	0.8	−1.2	19.2	2.7	5	6.1	1.1	2
II	15	1.5	−0.2	4.5	2.3	3	0.04	1	1
	16	2	−1	9.4	4.8	7	4.5	1.6	2
	17	1.5	−1	17.6	4.7	7	8.5	1.5	2

Table 5
Difference between two methods for T–C–S loading (zones *III* and *IV*).

Zone	Figure no.	S	R	Max. Value (%)	α	n	Min. Value (%)	α	n
III	18	−0.6	1	3.9	1	2	0.03	1.3	1
	19	−0.8	0.6	7.5	5	1	0.07	1.3	1
	20	−1	0.4	14.6	5	1	1.25	1.3	2
IV	21	−0.2	1	2.9	5	1	0.03	1.3	1
	22	−0.6	1.2	6.3	1	2	0.07	1.3	1
	23	−1	1.5	10.1	1	2	0.08	1.3	1

Please cite this article in press as: A. Jahanpour, F. Roozbahani, An applicable formula for elastic buckling of rectangular plates under biaxial and shear loads, Aerosp. Sci. Technol. (2016), http://dx.doi.org/10.1016/j.ast.2016.07.005

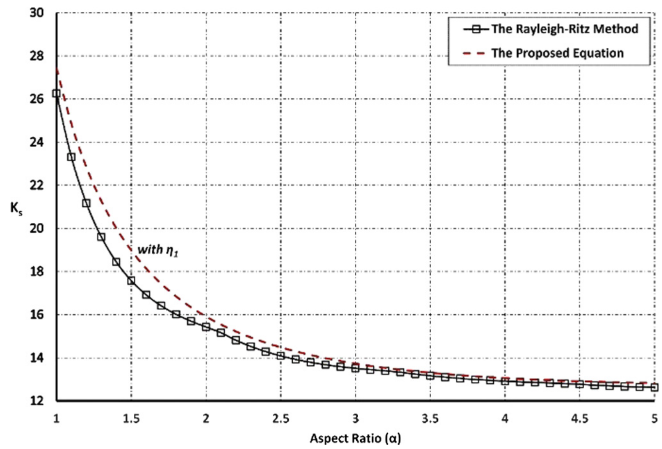

Fig. 24. The k_s–α diagrams for $S = -0.6$ and $R = -0.2$ (zone V).

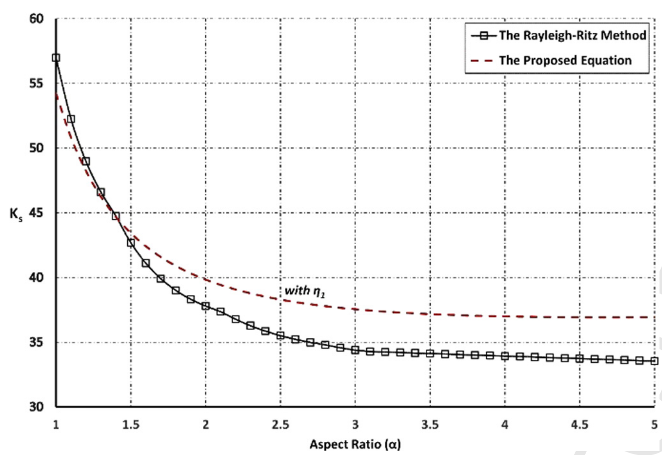

Fig. 25. The k_s–α diagrams for $S = -0.6$ and $R = -0.6$ (zone V).

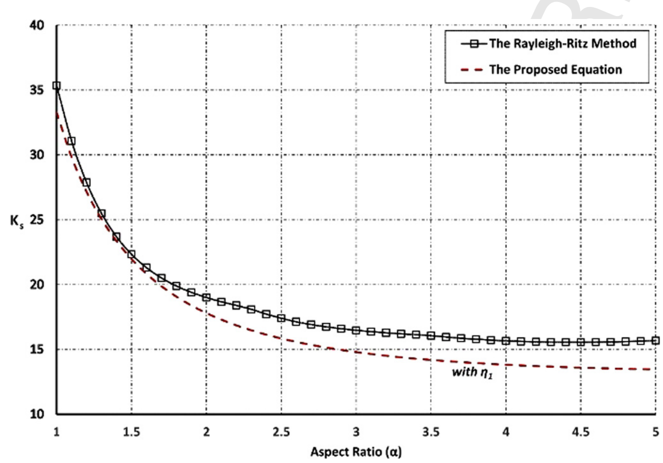

Fig. 26. The k_s–α diagrams for $S = -0.8$ and $R = -0.2$ (zone V).

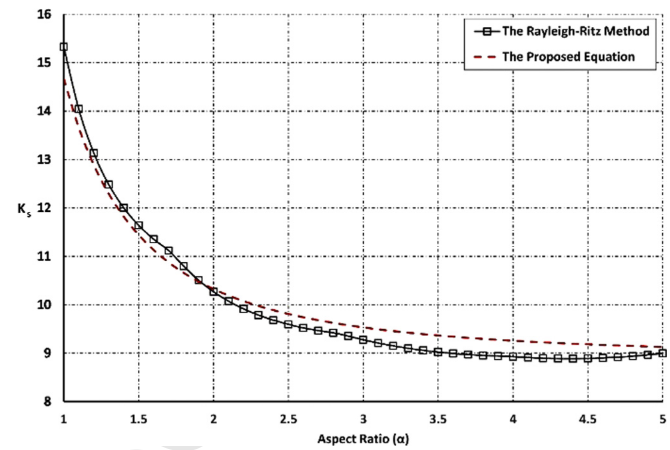

Fig. 27. The k_s–α diagrams for $S = -0.2$ and $R = -0.2$ (zone VI).

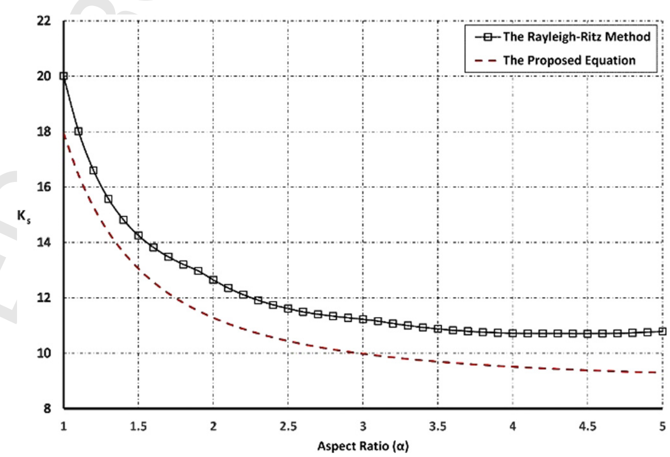

Fig. 28. The k_s–α diagrams for $S = -0.4$ and $R = -0.2$ (zone VI).

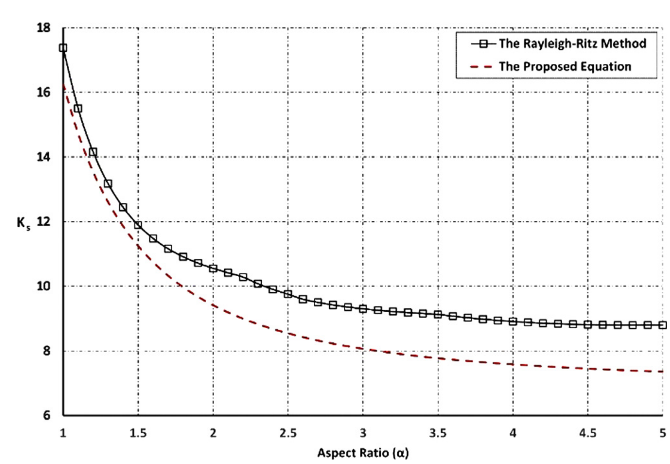

Fig. 29. The k_s–α diagrams for $S = -0.4$ and $R = -0.1$ (zone VI).

appeared maximum and minimum difference in Figs. 12–17 and 18–23 respectively. As seen in Table 4 and zone I (Figs. 12–14), increasing of $|R|$ leads to the error growing, so that for $|R| \geq 1$ it reaches to 19.2% rapidly (Fig. 14). Fig. 12 shows that Eq. (23) with the modifier factor (η_1) overestimates/underestimates values in the various aspect ratios. However, it is possible that for all of aspect ratio, the predicted values are always bigger than the actual ones (Fig. 13) or vice versa (Fig. 14). As the same way, in Figs. 15–17, the error reaches to 17.6%, when $|R| \geq 1$. In this zone, the estimated values are mostly smaller values than the actual ones.

In zones III and IV, the plate buckles transversely. Two or three modes may appear in the buckled plates as shown in Figs. 18–23. In zone III decreasing of 'R' leads to increasing of difference; but in zone IV with the shown Figs. 21–23, it is reversed. However, in these zones, the maximum errors are 14.6% (Fig. 20) and 10.1% (Fig. 23) respectively.

Please cite this article in press as: A. Jahanpour, F. Roozbahani, An applicable formula for elastic buckling of rectangular plates under biaxial and shear loads, Aerosp. Sci. Technol. (2016), http://dx.doi.org/10.1016/j.ast.2016.07.005

Table 6
Difference between two methods for T–T–S loading (zones V and VI).

Zone	Figure no.	S	R	Max.		Min.	
				Value (%)	α	Value (%)	α
V	24	−0.6	−0.2	8.5	1.3	0.9	3.3
	25	−0.6	−0.6	10.1	5	0.1	1.4
	26	−0.8	−0.2	14.2	5	1.4	1.4
VI	27	−0.2	−0.2	4.3	1	0.3	1.9
	28	−0.4	−0.2	13.9	5	7.7	1.3
	29	−0.4	−0.1	16.4	5	4.3	1.3

3.3. Tension–Tension–Shear loading (T–T–S)

There are two zones for this loading state: zone V in which modifier factor η_1 (Eq. (24)) must be used and zone VI in which Eq. (23) predicts explicitly acceptable results. In zone V one/both of the tensile stresses values are larger than 40% of the shear stress (Figs. 24–26) and otherwise, the loading state appears in zone VI (Figs. 27–29). It is pointed out both of zones should be considered with $m = n = 1$ and the obtained results have the required accuracy, when $|\sigma_y| \le |\sigma_x|$. If the latter condition is violated or stress ratios values ('S' and 'R') approach to unit, it is possible

Table 7
The comparison between FEM and two previous methods in C–C–S loading.

No.	α	β	τ (MPa)	σ_x (MPa)			$100\frac{C-B}{B}$%	$100\frac{A-B}{B}$%
				A	B	C		
				The Rayleigh–Ritz method	FEM	The proposed equation		
1	1	1.00	3.722	37.217	36.983	37.219	0.638	−0.634
2	1	0.20	12.349	61.747	61.360	61.747	0.631	−0.630
3	1	50.00	14.502	1.450	1.441	1.450	0.630	−0.635
4	1	1.00	35.687	35.687	35.457	35.668	0.594	−0.649
5	1	1.67	43.641	26.184	26.017	26.168	0.580	−0.642
6	1	2.50	49.012	19.605	19.476	19.587	0.570	−0.659
7	1	10.00	59.764	5.976	5.937	5.971	0.559	−0.658
8	1	1.00	75.217	30.087	30.035	30.269	0.779	−0.171
9	1	0.33	43.641	52.369	52.033	52.336	0.582	−0.645
10	1	0.25	99.848	39.939	39.664	39.935	0.683	−0.694
11	1	0.00	64.344	64.344	63.917	64.276	0.561	−0.668
12	1.5	1.00	2.688	26.884	26.704	26.882	0.665	−0.676
13	1.5	0.20	11.962	59.810	59.410	59.786	0.632	−0.674
14	1.5	50.00	7.671	0.767	0.763	0.767	0.652	−0.598
15	1.5	1.00	25.916	25.916	25.740	25.864	0.482	−0.685
16	1.5	1.67	29.249	17.549	17.429	17.504	0.427	−0.688
17	1.5	2.50	31.241	12.496	12.411	12.459	0.392	−0.690
18	1.5	10.00	34.760	3.476	3.452	3.463	0.322	−0.689
19	1.5	1.00	55.761	22.304	22.140	22.131	−0.038	−0.744
20	1.5	0.33	38.279	45.934	45.619	45.776	0.345	−0.691
21	1.5	0.25	83.800	33.520	33.276	33.569	0.879	−0.732
22	1.5	0.00	65.237	65.237	64.737	61.224	−5.427	−0.773
23	2	1.00	2.325	23.254	23.159	23.263	0.451	−0.410
24	2	0.20	12.279	61.393	60.955	61.388	0.711	−0.718
25	2	50.00	5.779	0.578	0.575	0.578	0.402	−0.466
26	2	1.00	22.616	22.616	22.507	22.418	−0.395	−0.486
27	2	1.67	24.462	14.677	14.606	14.526	−0.547	−0.490
28	2	2.50	25.499	10.200	10.150	10.085	−0.639	−0.493
29	2	10.00	27.225	2.723	2.709	2.687	−0.804	−0.502
30	2	1.00	49.906	19.962	19.854	19.532	−1.619	−0.547
31	2	0.33	38.087	45.704	45.474	44.851	−1.370	−0.506
32	2	0.25	80.970	32.388	32.103	31.493	−1.901	−0.887
33	2	0.00	57.898	57.898	57.422	56.554	−1.511	−0.829
34	3	1.00	2.067	20.666	20.630	20.679	0.238	−0.174
35	3	0.20	11.914	59.568	59.240	59.539	0.505	−0.554
36	3	50.00	4.584	0.458	0.457	0.458	0.145	−0.259
37	3	1.00	20.333	20.333	20.283	19.949	−1.645	−0.245
38	3	1.67	21.150	12.690	12.659	12.431	−1.808	−0.242
39	3	2.50	21.588	8.635	8.613	8.449	−1.900	−0.258
40	3	10.00	22.267	2.227	2.222	2.176	−2.045	−0.235
41	3	1.00	46.744	18.698	18.645	17.382	−6.771	−0.284
42	3	0.33	36.771	44.125	43.836	44.413	1.317	−0.658
43	3	0.25	73.820	29.528	29.309	30.649	4.573	−0.748
44	3	0.00	56.051	56.051	55.610	54.299	−2.358	−0.794
45	5	1.00	1.936	19.361	19.341	19.356	0.077	−0.103
46	5	0.20	11.770	58.851	58.465	58.825	0.616	−0.661
47	5	50.00	4.023	0.402	0.402	0.402	−0.017	−0.116
48	5	1.00	19.214	19.214	19.195	18.681	−2.678	−0.098
49	5	1.67	19.512	11.707	11.695	11.371	−2.769	−0.106
50	5	2.50	19.664	7.866	7.857	7.636	−2.814	−0.114
51	5	10.00	19.897	1.990	1.987	1.930	−2.885	−0.121
52	5	1.00	46.024	18.409	18.389	16.454	−10.520	−0.112
53	5	0.33	36.260	43.513	43.247	43.961	1.651	−0.614
54	5	0.25	70.711	28.284	28.078	31.136	10.891	−0.734
55	5	0.00	55.156	55.156	54.716	52.866	−3.382	−0.804

Please cite this article in press as: A. Jahanpour, F. Roozbahani, An applicable formula for elastic buckling of rectangular plates under biaxial and shear loads, Aerosp. Sci. Technol. (2016), http://dx.doi.org/10.1016/j.ast.2016.07.005

Table 8
The comparisons between FEM and two previous methods in T–C–S and T–T–S loadings.

No.	α	S	R	σ_x (MPa) A Rayleigh–Ritz method	B Finite element model	C Proposed equation	$100\frac{C-B}{B}$ %	$100\frac{A-B}{B}$ %
1	1	1	−1	124.927	124.420	126.789	1.904	−0.407
2	1	−1	1	−124.927	−124.420	−126.789	1.904	−0.407
3	1	−0.6	1	−66.019	−65.790	−66.355	0.858	−0.349
4	1	1	−0.6	110.032	109.650	105.750	−3.557	−0.349
5	1	−0.2	−0.2	−57.083	−56.710	−54.625	−3.676	−0.657
6	1.5	1	−1	112.229	111.520	109.846	−1.501	−0.636
7	1.5	−1	1	−57.343	−57.044	−56.990	−0.095	−0.525
8	1.5	−0.6	1	−28.039	−27.756	−27.871	0.415	−1.019
9	1.5	1	−0.6	87.989	86.950	88.063	1.280	−1.195
10	1.5	−0.2	−0.2	−43.343	−42.924	−42.598	−0.760	−0.975
11	3	1	−1	103.051	102.190	97.186	−4.897	−0.842
12	3	−1	1	−25.190	−24.930	−24.520	−1.645	−1.044
13	3	−0.6	1	−14.422	−14.256	−14.075	−1.268	−1.161
14	3	1	−0.6	83.707	83.620	80.430	−3.815	−0.103
15	3	−0.2	−0.2	−34.529	−34.426	−35.486	3.079	−0.299
16	5	1	−1	99.792	99.213	96.814	−2.418	−0.584
17	5	−1	1	−20.778	−20.540	−20.163	−1.834	−1.157
18	5	−0.6	1	−12.266	−12.126	−11.908	−1.797	−1.151
19	5	1	−0.6	80.746	79.910	80.244	0.417	−1.047
20	5	−0.2	−0.2	−32.704	−32.252	−33.996	5.409	−1.403

that the plate yielding occurs before the elastic buckling. For example, in Fig. 25, which $S = R = -0.6$, the minimum k_s for the big aspect ratios is converged to about 35. For mild steel material with $E = 206$ GPa, $\nu = 0.3$ and $F_y = 240$ MPa, it can be easily shown that if $b/t > 217$, then the elastic buckling is prior to the plate yielding. The obtained thickness ratio is big enough to have a membranous plate.

The maximum and minimum differences in Figs. 24–26 (zone V) and Figs. 27–29 (zone VI) have been shown in Table 6. The occurred errors in Fig. 24 is relatively small and they may increase with overestimated values (Fig. 25) or underestimated values (Fig. 26). Also, in Fig. 27, there is good conformity between two diagrams (Table 6); but the significant underestimated values have been predicted in Figs. 28 and 29. It seems that there is not a rational relationship between the load ratios ('S' and 'R') and the appeared differences. The maximum error in zones V and VI are 14% and 16% respectively.

4. Validation of the results with finite element method

Tables 7 and 8 summarize the results of some examples that are caught from finite element modeling and two previous methods. The Eigen-buckling analysis is applied on the FE modeling. The used element is 8-nodes SHELL with 5 degree of freedom. The convergence conditions shows that the element dimension should be 2 cm. All of models have 1 m width and 10 mm thickness with $E = 206$ GPa, $\nu = 0.3$ and the reference stress $\sigma_e = \frac{\pi^2 D}{tb^2} = 18.618$ MPa. The σ_x values are calculated from three methods (The Rayleigh–Ritz method, FEM and Eq. (19) or (23)) for some aspect ratios and load ratios. They have been shown in Tables 7 and 8 for C–C–S and C–T–S/T–T–S states respectively. Tables 7 and 8 show that the maximum difference between the proposed equation and FEM is less than 11% and between the Rayleigh–Ritz method and FEM is about 1.4%.

5. Conclusion

In this paper, using the Rayleigh–Ritz method, the buckling load of a simply supported rectangular plate under biaxial and shear loads was evaluated. The plate aspect ratio was supposed that varies from 1 to 5 and with several loading states, 15 129 examples were considered. Then, applying the regression techniques and interpolation on the obtained data, a concise equation (Eq. (19) or (23)) is approximated to predict the buckling load coefficient. It can be shown that for longer plates ($\alpha > 5$), the obtained results for $\alpha = 5$ are applicable with a good accuracy. In Compression–Compression–Shear state, the maximum error in the proposed equation increases when the aspect ratio rises. However, it is always less than 8% ($3 \le \alpha \le 5$).

In presence of tensile stress(es), right hand of the proposed equation must be always considered unit. When the tensile stress (σ_y) is applied on the plate length (the longer direction) and the compressive stress, $\sigma_x \le 1.4\tau$, then a modifier factor (η_1) must be applied on the results. Furthermore, if the tensile stress (σ_x) is applied on the plate width and its value is larger than 40% of the shear stress and also $\sigma_y \le \tau$, then another modifier factor (η_2) must be used. The predicted results by the proposed equation lead to error up to 20% in some states.

The proposed equation is directly applicable for Tension–Tension–Shear state, when both of tensile stresses values are less than 40% of the shear stress; otherwise, the modifier factor, η_1 should be used to decrease errors. However, the maximum appeared error reaches to 16%. Finally, the achieved results from two methods were compared with those of FEM; thus the maximum difference between the Rayleigh–Ritz method and FEM is about 1.4%.

Conflict of interest statement

None declared.

References

[1] P.S. Bulson, The Stability of Flat Plates, Chatto and Windus, London, 1970.
[2] S. Timoshenko, J. Gere, Theory of Elastic Stability, 2nd edition, McGraw-Hill, New York, 1985.
[3] F. Bloom, Handbook of Thin Plate Buckling and Post-buckling, Chapman & Hall/CRC, Boca Raton (Fla), 2001.
[4] C. Libove, Buckled pattern of biaxially compressed simply supported orthotropic rectangular plates, J. Compos. Mater. 17 (1) (1983) 45–48.
[5] A. van der Neut, Buckling caused by thermal stresses, in: High Temperature Effects in Aircraft Structures, in: AGARDograph, vol. 28, 1958, pp. 215–247.
[6] M.B. Benoy, An energy solution to the buckling of rectangular plates under non-uniform in-plane loading, Aeronaut. J. 73 (1969) 974–977.
[7] C.W. Bert, K.K. Devarakonda, Buckling of rectangular plates subjected to nonlinearly distributed in-plane loading, Int. J. Solids Struct. 40 (2003) 4097–4106.
[8] L.C. Bank, J. Yin, Buckling of orthotropic plates with free and rotationally re-

Please cite this article in press as: A. Jahanpour, F. Roozbahani, An applicable formula for elastic buckling of rectangular plates under biaxial and shear loads, Aerosp. Sci. Technol. (2016), http://dx.doi.org/10.1016/j.ast.2016.07.005

strained unloaded edges, Thin-Walled Struct. 24 (1996) 83–96.

[9] J. Kang, A. Leissa, Vibration and buckling of SS-F-SS-F rectangular plates loaded by in-plane moments, Int. J. Struct. Stab. Dyn. 1 (4) (2001) 527–543.

[10] P.T. Elangovan, M. Prinsze, Critical shear stress of flat rectangular plates with free edges, Thin-Walled Struct. 13 (1992) 409–425.

[11] A.N. Sherbourne, M.D. Pandey, Differential quadrature method in the buckling analysis of beams and composite plates, Comput. Struct. 40 (4) (1991) 903–913.

[12] O. Civalek, Application of differential quadrature (DQ) and harmonic differential quadrature (HDQ) for buckling analysis of thin isotropic plates and elastic columns, Eng. Struct. 26 (2004) 171–186.

[13] K.M. Liew, X.L. Chen, J.N. Reddy, Mesh-free radial basis function method for buckling analysis of non-uniformly loaded arbitrarily shaped shear deformable plates, Comput. Methods Appl. Mech. Eng. 193 (2004) 205–224.

[14] O. Civalek, A. Korkmaz, Ç. Demir, Discrete singular convolution approach for buckling analysis of rectangular Kirchhoff plates subjected to compressive loads on two opposite edges, Adv. Eng. Softw. 41 (2010) 557–560.

[15] K.I. McKenzie, The buckling of rectangular plate under combined biaxial compression, bending and shear, Aeronaut. Q. 15 (3) (1964) 239–246.

[16] Y.G. Liu, M.N. Pavlovic, A generalized analytical approach to the buckling of simply-supported rectangular plates under arbitrary loads, Eng. Struct. 30 (2008) 1346–1359.

[17] M. Stein, J. Neff, Buckling stresses of simply supported rectangular flat plates in shear, NACA, TN 1222, 1947.

[18] S.B. Batdorf, M. Stein, Critical combinations of shear and direct stress for simply supported rectangular flat plates, NACA TN 1223, 1947.

[19] V. Piscopo, Buckling analysis of rectangular plates under the combined action of shear and uniaxial stresses, World Acad. Sci., Eng. Technol. 46 (2010) 546–553.

[20] H. Wagner, About Construction and Calculation Questions of Sheet Construction, W.G.L. Yearbook, 1928, pp. 113–125 (in German).

[21] O.S. Heck, H. Ebner, Methods and formulas for calculating the strength of plate and shell construction as used in airplane design, NACA TM 785, 1936.

[22] W.C. Young, R.G. Budynas, Roark's Formulas for Stress and Strain, seventh edition, McGraw-Hill, New York, 2002.

[23] Y.Z. Chen, Y.Y. Lee, Y.J. Guo, Concise formula for the critical buckling stresses of an elastic plate under biaxial compression and shear, J. Constr. Steel Res. 65 (2009) 1507–1510.

[24] Buckling strength of plated structures. Recommended practice, DNV-RP-C201, October 2010.

[25] F. Roozbahani, Evaluation of buckling behavior of rectangular plates under in-plane loads, M.Sc. thesis, Malayer University, Feb. 2015.

[26] GeneXproTools, version 4, Time Limited Trial, Online User's Manual, Gepsoft, 2008.

Please cite this article in press as: A. Jahanpour, F. Roozbahani, An applicable formula for elastic buckling of rectangular plates under biaxial and shear loads, Aerosp. Sci. Technol. (2016), http://dx.doi.org/10.1016/j.ast.2016.07.005